

Single-Dirac-cone Z_2 topological insulator phases in distorted Li_2AgSb -class and related quantum critical Li-based spin-orbit compounds

H. Lin,¹ L.A. Wray,² Y. Xia,² S.-Y. Xu,² S. Jia,³ R.J. Cava,³ A. Bansil,¹ and M.Z. Hasan^{2,4,5}

¹*Department of Physics, Northeastern University, Boston, Massachusetts 02115, USA*

²*Joseph Henry Laboratories of Physics, Princeton University, Princeton, New Jersey 08544, USA*

³*Department of Chemistry, Princeton University, Princeton, New Jersey 08544, USA,*

⁴*Princeton Center for Complex Materials, Princeton University, Princeton, New Jersey 08544, USA*

⁵*Princeton Institute for Science and Technology of Advanced Materials,*

*PRISM, Princeton University, Princeton, New Jersey 08544, USA**

(Dated: April 6, 2010)

We have extended our new materials class search for the experimental realization of Z_2 topological insulators from binary [**Bi₂Se₃ class**, Xia *et.al.*, Nature Phys.**5**, 398 (2009)] and the ternary [**Half-Heusler class**, Lin *et.al.*, arXiv:1003.0155 (2010)] series to non-Heusler **Li-based ternary intermetallic series** $\text{Li}_2M'X$ ($M'=\text{Cu, Ag, and Au}$, $X=\text{Sb and Bi}$) with CuHg_2Ti -type structure. We discovered that the distorted- Li_2AgSb is a lightweight compound harboring a 3D topological insulator state with $Z_2=-1$ although the groundstate lies near a critical point, whereas the related Li_2CuSb -type compounds are topologically trivial. Non-Heusler ternary $\text{Li}_2M'X$ series (with a number of variant compounds) we identified here is a new platform for deriving novel stoichiometric compounds, artificial quantum-well/heterostructures, nano-wires, nano-ribbons and nanocrystals. We have grown some of these bulk materials (experimental results will be reported separately).

PACS numbers:

Topological insulators (TI)[1–10] realize a novel state of quantum matter that are distinguished by topological invariants of bulk band structure rather than spontaneously broken symmetries. Its material realization in 2D artificial HgTe-quantum wells [8] and 3D Bi-based binary compounds [9–18] led to a surge of interest in discovering novel topological physics in world-wide condensed matter community. A number of exotic quantum phenomena have been predicted to exist in multiply-connected geometries [19–25] which require an enormous amount of materials flexibility. Given the right materials, these topological properties naturally open a window to new realms of spintronics and quantum computing. Just as the majority of normal metals are neither good superconductors nor strongly magnetic, there is no inherent likelihood that the band structure of topological insulators known so far will be suitable for the realization of any of the novel physical states or devices that have been predicted for quantum computing or spintronics. We need to expand our search. We have extended our previous search for TI materials from binary (Bi_2X_3 series, Xia *et.al.*, Nature Phys. **5**, 398 (2009)) and the thermoelectric ternary compounds (half-Heuslers, Lin *et.al.*, arXiv:1003.0155[26]) to $\text{Li}_2M'X$ ($M'=\text{Cu, Ag, and Au}$, $X=\text{Sb and Bi}$) series. We discover that the distorted Li_2AgSb is the best lightweight ternary compound of the “ $M_2M'X$ ” series harboring a 3D topological insulator state with $Z_2=-1$. We also show that the $\text{Li}_2M'X$ series is a natural platform that hosts a range of candidate compounds, alloys and artificial heterostructures (quantum-

wells). We also discovered several different paradigms of trivial and non-trivial topological ordering in this class, including an intrinsically metallic nontrivial topological state in Li_2AgBi and Li_2AuBi . In this Letter, we use first principles theoretical calculations to show that distorted Li_2AgSb is the best lightweight ternary compound expected to realize a three dimensional topological insulator state.

The crystal lattice of $\text{Li}_2M'X$ ($M'=\text{Cu, Ag, and Au}$, $X=\text{Sb and Bi}$) is described by the space group $F\bar{4}3m$, with the atomic arrangement presented in Fig. 1A. M' and X atoms occupy the Wyckoff 4d and 4a positions, respectively. Li atoms fill the remaining empty space in 4b and 4c positions. Because M' and X atoms form a zincblende type sublattice, these materials resemble the topologically nontrivial gray tin. There is no spatial inversion symmetry in $\text{Li}_2M'X$ compounds. These observations suggest that $\text{Li}_2M'X$ could be candidates for 3D Z_2 topological insulators if some odd number of band inversions are realized.

First-principles band calculations were performed with the linear augmented-plane-wave (LAPW) method using the WIEN2K package [28] in the framework of density functional theory (DFT). The generalized gradient approximation (GGA) of Perdew, Burke, and Ernzerhof [29] was used to describe the exchange-correlation potential. Spin orbital coupling (SOC) was included as a second variational step using a basis of scalar-relativistic eigenfunctions. The calculated (DFT-GGA) band structures of Li_2AgSb , Li_2AgBi , Li_2AuBi , and Li_2CuSb along high symmetry lines in the Brillouin zone are presented in Fig. 5. A common feature of these materials is that the top of the valence band is located at the Γ -point. For Li_2AgSb , away from Γ , the Fermi level is completely

*Electronic address: mzhasan@Princeton.edu

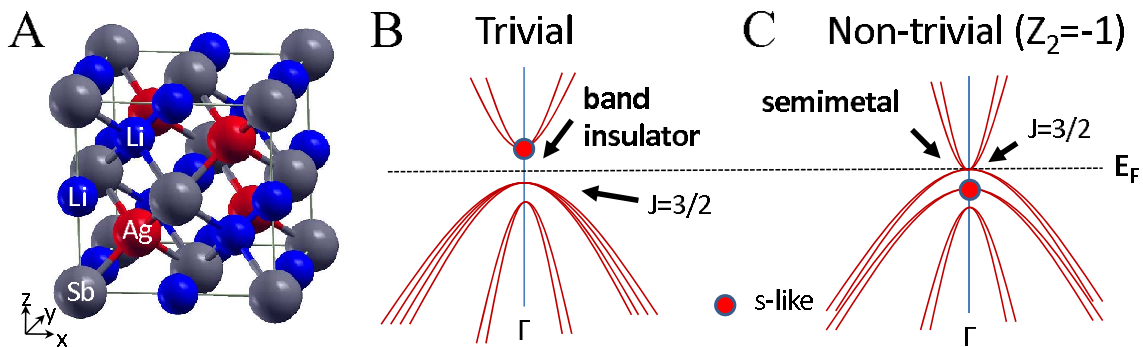


FIG. 1: **Li₂AgSb crystal structure and topological band inversion:** **a** The crystal structure of Li₂AgSb. Li, Ag, and Sb are denoted by blue, red, and gray balls. Sb and Ag form the zinc-blende structure. Diagrams in **b-c** illustrate band structures near the Γ -point for trivial and non-trivial cases, respectively. Red dots denote the *s*-like orbitals at Γ -point. Band inversion occurs in the non-trivial case where the *s*-like orbitals at the Γ -point are below the four-fold degenerate $j = 3/2$ bands.

gapped. Therefore, the topological properties can be determined from observations of band structure only near the Γ -point. For Li₂AgBi and Li₂AuBi, part of the conduction band along L- Γ is below the E_F and forms electron pockets near the L-point. The conduction band and valence band overlap and the topological index Z_2 is not well defined. If the overlap is removed by distortion, Z_2 can also be determined from the band structure only near the Γ -point.

Confining our view to band structure very close to the Fermi level (Fig. 5a(inset)), we find that the orbital angular momentum symmetries of Li₂M'X compounds are identical to those defining low energy properties in HgTe and CdTe. For Li₂AgBi and Li₂AuBi, two upward-concave bands and two downward-concave bands are degenerate at the Γ point. These four-fold degenerate states at the Γ -point have *p*-type orbital symmetry with a total angular momentum eigenvalue of $j = 3/2$, and lie above a two-fold degenerate *s*-like state, representing an inversion relative to the natural order of *s*- and *p*-type orbital derived band structure. Away from the Γ -point, the upward dispersing bands gain significant *s*-like character due to orbital hybridization. Thus, by analogy with HgTe, we expect Li₂AgBi and Li₂AuBi to be a topologically nontrivial metal (or “topological metal”), as is the case with elemental antimony [11], and its conductivity could probably be manipulated through alloying, just as antimony was alloyed with bismuth to discover the first known example of a three dimensional TI [9] (Bi_{1-x}Sb_x). The *s*-type bands in Li₂CuSb are above E_F and above the $j = 3/2$ bands, meaning that its band structure lacks the *s/p* inversion that leads to strong topological order. For Li₂AgSb, the *s*-type and *p*-type states at the Γ -point is nearly degenerate. The conduction band and one of the valence band have almost linear dispersion around the Γ -point, indicating it is on the critical point of the topological phase. With a small expansion of lattice, the *s/p* band inversion occurs as shown in Fig. 3(b). As we will establish more rigorously below, these symmetries correctly indicate that Li₂CuSb is topologically trivial

while expanded Li₂AgSb is topologically nontrivial.

In terms of the symmetry notation that has been applied to HgTe in previous literature, our calculations show that bands near E_F at the Γ -point possess Γ_6 (2-fold degenerate), Γ_7 (2-fold degenerate), and Γ_8 (4-fold degenerate) symmetry in all of these compounds. Both expanded Li₂AgSb and HgTe have Γ_8 states at E_F . The Γ_6 symmetry bands are below Γ_8 and occupied, providing the band inversion that distinguishes topological order. Although the order of Γ_7 and Γ_6 is different, it is not relevant to the topological nature since both are occupied. In the band structures of topologically trivial band insulators Li₂CuSb and CdTe, the Γ_6 states are above the downward dispersing valence bands. These non-inverted Γ_6 states lie above E_F and are unoccupied. It is due to the occupancy of Γ_6 bands at the Γ -point in Li₂AgSb that the Z_2 topological invariant picks up an extra factor of -1 when compared to Li₂CuSb.

The fact that none of the topologically nontrivial materials discussed in this work (3D-HgTe, expanded Li₂AgSb, Li₂AgBi, and Li₂AuBi) are naturally insulating known to be due to the Γ -point degeneracy of positive- and negative-mass bands with Γ_8 symmetry, which results from the crystal symmetry group. Distortion of the crystal lattice through static pressure or finite size effects can lift the degeneracy and open a gap at E_F , causing a direct gap between the topologically inverted valence and conduction bands and resulting in the appearance of topologically defined surface states. Fu and Kane have previously discussed this possibility for 3D-HgTe[4]. In Fig. 5c, we demonstrate that a perturbative rhombohedral lattice distortion caused by uniaxial pressure will lift the band structure degeneracy in Li₂AgSb, resulting in a fully gapped topological insulator state. With reference to the convention cubic structure, a 3% expansion is applied in the plane perpendicular to [111]. As has been observed when distortion is applied to the zincblende structured binary compound HgTe, bulk band structure of the distorted Li₂AgSb is fully gapped and realizes strong Z_2 topological order.

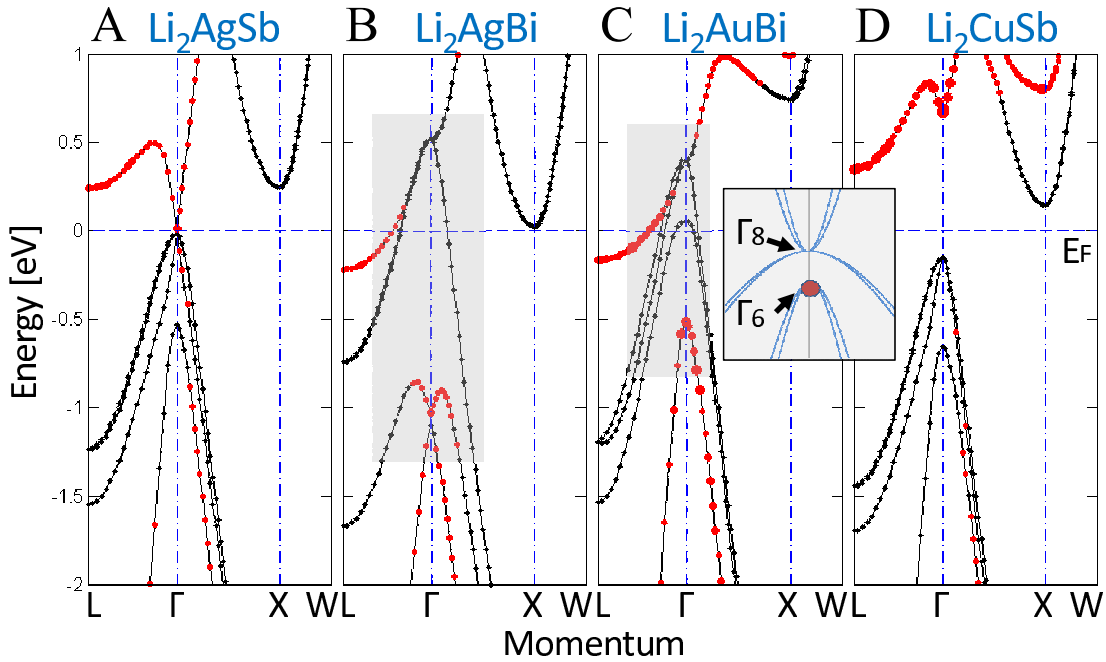


FIG. 2: **Li₂M'X electronic structures**: Bulk band structures of (a) Li₂AgSb, (b) Li₂AgBi, (c) Li₂AuBi, and (d) Li₂CuSb. The size of red data points is proportional to the probability of s-orbital occupation on the anion atom (“X”). An inset in panel c highlights inverted band symmetries associated with topological order, corresponding to the diagram in Fig. 1c.

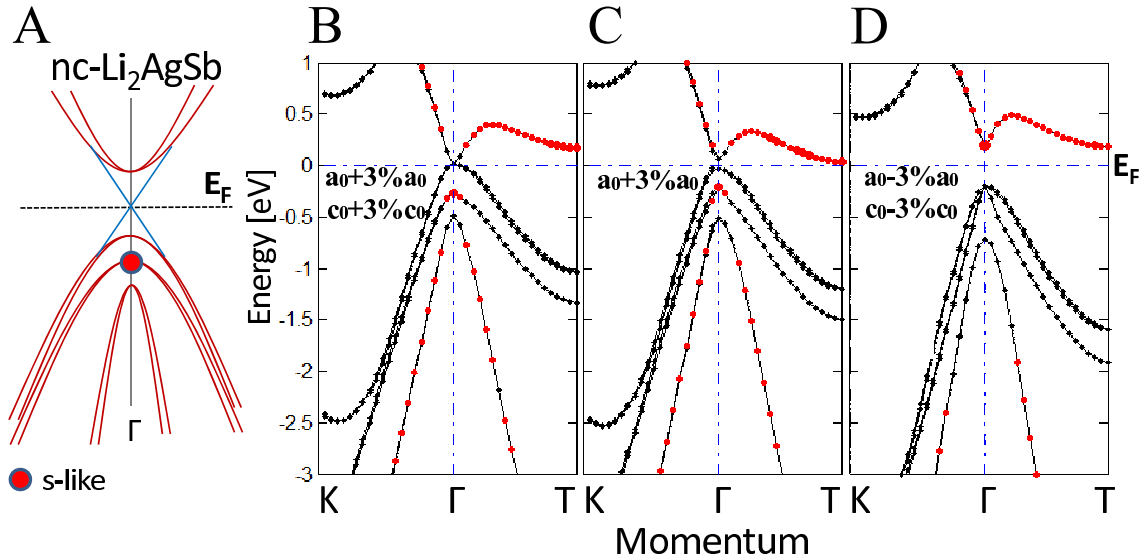


FIG. 3: **Topological insulator state with a single-Dirac-cone**: (a) A sketch of band structure near the Γ -point for topologically non-trivial Li₂AgSb with a lattice distortion. The s-like Γ_6 states are marked with a red dot. Lattice distortion causes a gap to open at E_F , resulting in a topological insulator state. For such a topological insulator, the surface bands will span the bulk band gap and should have an odd number of Dirac cones, resembling the dispersion plotted with blue lines. (b) Band structures of expanded Li₂AgSb where $a = a_0 + 3\%a_0$ and $c = c_0 + 3\%c_0$, where a_0 and c_0 correspond to the experimental lattice. (c) Band structures of rhombohedral distorted Li₂AgSb with lattice constants $a = a_0 + 3\%a_0$ and $c = c_0$ (d) Band structures of Li₂AgSb under hydrostatic pressure where $a = a_0 - 3\%a_0$ and $c = c_0 - 3\%c_0$.

Conversely, the topological band inversion in Li₂AgSb can be removed altogether by uniformly decreasing all lattice constants, demonstrating the sensitive chemical tunability in this TI class (Fig. 5d). After a 3% reduction in all lattice parameters, the s-like Γ_6 symmetry bands

are observed to rise above the Γ_8 bands, removing band inversion at the Γ -point and resulting in a topologically trivial band insulator state.

In conclusion, we have discovered a new class of topological insulator materials realized by distorted

$\text{Li}_2M'X$, and demonstrated band structure topology calculations for representative topologically critical semimetal (Li_2SbAg) and nontrivial metallic (Li_2AgBi

and Li_2AuBi) materials. Bulk band structure in distorted Li_2SbAg is shown to be characterized by $Z_2=-1$.

-
- [1] For a brief review see: J.E. Moore, The Birth of Topological Insulators, *Nature* **464**, 194 (2010). <http://dx.doi.org/10.1038/nature08916>
- [2] Kane, C. L. & Mele, E. J. Z_2 Topological Order and the Quantum Spin Hall Effect. *Phys. Rev. Lett.* **95**, 146802 (2005).
- [3] Bernevig B. A., Hughes T. L., Zhang S.-C. Quantum spin Hall effect and topological phase transition in HgTe quantum wells. *Science* **314**, 1757 (2006).
- [4] Fu, L. and C.L. Kane Topological Insulators with Inversion Symmetry. *Phys. Rev. B* **76**, 045302 (2007).
- [5] Fu, L., Kane, C. L., & Mele, E. J. Topological insulators in three dimensions. *Phys. Rev. Lett.* **98**, 106803 (2007).
- [6] Moore, J. E. & Balents, L. Topological invariants of time-reversal-invariant band structures. *Phys. Rev. B* **75**, 121306(R) (2007).
- [7] Roy, R. Topological phases and the quantum spin Hall effect in three dimensions, *Phys. Rev. B* **79**, 195322 (2009).
- [8] Konig, M. *et al.* Quantum spin Hall insulator state in HgTe quantum wells. *Science* **318**, 766 (2007).
- [9] Hsieh, D. *et al.* A topological Dirac insulator in a quantum spin Hall phase. *Nature (London)* **452**, 970 (2008).
- [10] Hsieh, D. *et al.* A tunable topological insulator in the spin helical Dirac transport regime. *Nature (London)* **460**, 1101 (2009).
- [11] Hsieh, D. *et al.* Observation of unconventional quantum spin textures in topological insulators. *Science* **323**, 919 (2009).
- [12] Xia, Y. *et al.* Observation of a large-gap topological-insulator class (Bi_2Se_3 class) with a single Dirac cone on the surface. *Nature Phys.* **5**, 398 (2009). <http://dx.doi.org/10.1038/nphys1294>
- [13] Zhang, H. *et al.* Topological insulators in Bi_2Se_3 , Bi_2Te_3 and Sb_2Te_3 with a single Dirac cone on the surface. *Nature Phys.* **5**, 438 (2009).
- [14] Roushan, P. *et al.* Topological surface states protected by chiral spin textures *Nature (London)* **460**, 1106 (2009).
- [15] Noh, H.-J. *et al.*, Spin-orbit interaction effect in the electronic structure of Bi_2Te_3 observed by angle-resolved photoemission spectroscopy, *Europhys. Lett.* **81**, 57006 (2008).
- [16] Chen, Y.L. *et al.*, Realization of a Three Dimensional Topological Insulator Bi_2Te_3 , *Science* **325**, 178 (2009).
- [17] Hsieh, D. *et al.* Observation of time-reversal-protected single-Dirac-cone spin-polarized topological-insulator states in Bi_2Te_3 and Sb_2Te_3 . *Phys. Rev. Lett.* **103**, 146401 (2009).
- [18] Wray, L.A. *et al.* Observation of unconventional band topology in a superconducting doped topological insulator $\text{Cu}_x\text{-Bi}_2\text{Se}_3$. Preprint at (<http://arxiv.org/abs/0912.3341>) (2009).
- [19] Fu, L. and C.L. Kane Superconducting proximity effect and Majorana fermions at the surface of a topological insulator, *Phys. Rev. Lett.* **100**, 096407 (2008).
- [20] Fu, L. & Kane, C. L. Probing neutral Majorana fermion edge modes with charge transport. *Phys. Rev. Lett.* **102**, 216403 (2009).
- [21] Qi X.-L. *et al.* Inducing a magnetic monopole with topological surface states. *Science* **323**, 1184 (2009)
- [22] Teo, J. C.Y. & Kane, C. L. Majorana fermions and non-Abelian statistics in three dimensions. *Phys. Rev. Lett.* **104**, 046401 (2010).
- [23] Lee, D.-H. Surface States of Topological Insulators: The Dirac Fermion in Curved Two-Dimensional Spaces. *Phys. Rev. Lett.* **103**, 196804(2009).
- [24] Law, K. P.A. Lee, T. Ng, Majorana Fermion Induced Resonant Andreev Reflection. *Phys. Rev. Lett.* **103**, 237001 (2009).
- [25] Xu, C. Quantum critical points of helical Fermi liquids. *Physical Review B* **81** 054403 (2010).
- [26] Lin, H. *et al.*, A new platform for topological quantum phenomena : Topological Insulator states in thermoelectric Heusler-related ternary compounds. arXiv:1003.0155 (2010).
- [27] Wyckoff, R. W. G. Crystal Structures (Krieger, Melbourne, FL, 1986), Vol. 2.
- [28] Blaha, P., K. Schwarz, G. K. H. Madsen, D. Kvasnicka, and J. Luitz, WIEN2k, An Augmented Plane Wave Plus Local Orbitals Program for Calculating Crystal Properties, (Karlheinz Schwarz, Techn. University Wien, Austria), 2001. ISBN 3-9501031-1-2.
- [29] Perdew, P. et al., *Phys. Rev. Lett.* **77**, 3865 (1996).

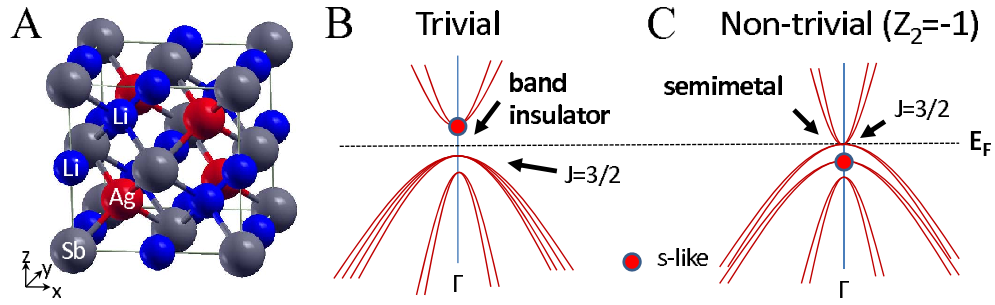


FIG. 4: **Li₂AgSb crystal structure and band inversion:** **a** The crystal structure of Li₂AgSb. Li, Ag, and Sb are denoted by blue, red, and gray balls. Sb and Ag form the zinc-blende structure. Diagrams in **b-c** illustrate band structures near the Γ -point for trivial and non-trivial cases, respectively. Red dots denote the s-like orbitals at Γ -point. Band inversion occurs in the non-trivial case where the s-like orbitals at the Γ -point are below the four-fold degenerate $j = 3/2$ bands.

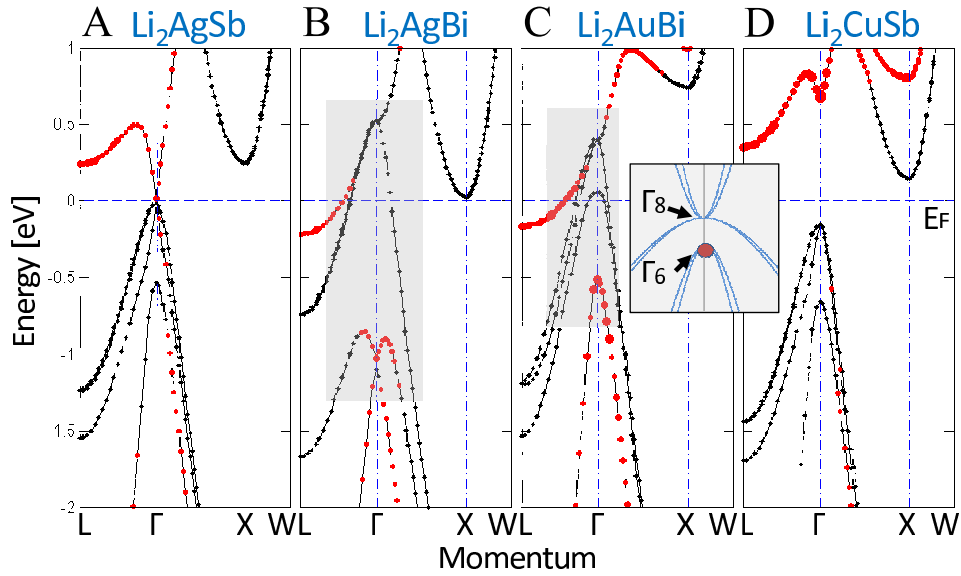


FIG. 5: **Li₂M'X band structures:** Bulk band structures of (a) Li₂AgSb, (b) Li₂AgBi, (c) Li₂AuBi, and (d) Li₂CuSb. The size of red data points is proportional to the probability of s-orbital occupation on the anion atom (“X”). An inset in panel c highlights inverted band symmetries associated with topological order, corresponding to the the diagram in Fig. 1c.

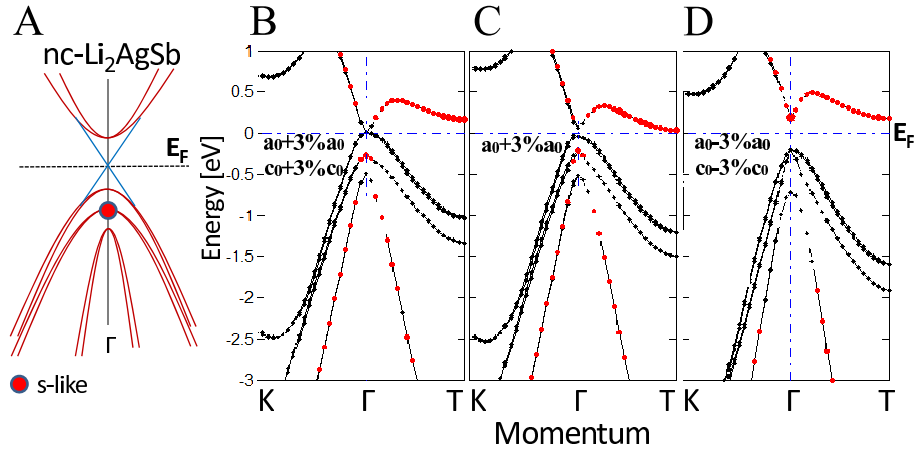


FIG. 6: **The topological insulator state with a single-Dirac-cone:** (a) A sketch of band structure near the Γ -point for topologically non-trivial Li₂AgSb with a lattice distortion. The s-like Γ_6 states are marked with a red dot. Lattice distortion causes a gap to open at E_F , resulting in a topological insulator state. For such a topological insulator, the surface bands will span the bulk band gap and should have an odd number of Dirac cones, resembling the dispersion plotted with blue lines. (b) Band structures of expanded Li₂AgSb where $a = a_0 + 3\%a_0$ and $c = c_0 + 3\%c_0$, where a_0 and c_0 correspond to the experimental lattice. (c) Band structures of rhombohedral distorted Li₂AgSb with lattice constants $a = a_0 + 3\%a_0$ and $c = c_0$ (d) Band structures of Li₂AgSb under hydrostatic pressure where $a = a_0 - 3\%a_0$ and $c = c_0 - 3\%c_0$.